

# Fault Diagnosis of the Aeroengine Based on Neural Network and D-S Evidence Theory

WenJie Wu, DaGui HUANG and Zheng DONG

School of Mechatronics Engineering, University of Electronic Science and Technology of China, Chengdu, China

**Abstract**—This paper describes a new fusion algorithm based on Dempster-Shafer theory of evidence and neural networks. D-s theory is applied to the diagnosis data fusion for the sub-systems with BP neural network, probability neural network, radial neural network and Elman neural network methods. The simulation of the anti-noise ability for the test system is analyzed. The results manifest that the standardization of the samples influence the neural network training and anti-noise ability. Compared with the approaches that only adopt D-S evidence theory or neural network, the accuracy of diagnosis result is obviously improved. It has better system function, validity and accuracy of fault diagnosis for the aeroengine.

**Keywords**-aeroengine; data fusion; D-S theory; fault diagnosis; neural network;

## 1. Introduction

Artificial Neural Networks have proven effective in solving problems in a wide variety of areas, such as the fault diagnosis and working state monitor of aeroengine[1],[2]. And it is widely applied in the last two decades. Fault diagnosis of aeroengine based on neural network and D-S evidence theory was researched in America [3],[4]. Recently, a lot of engine fault diagnosis research has been made in China, and they got good test results [5]-[7]. An engine is a general power source, its reliability is very important[8]. Its structure is very complex and its work condition is very bad, so the occurrence of failures become obvious. Unfortunately with the complexity of the aeroengine, the bad test environment and the noise interference, it makes the application of artificial neural network or expert system fault diagnosis method limited because of the misdiagnosis or missed diagnosis[9]. Therefore, to improve the fault diagnosis accuracy and the anti-noise ability become the hot research topic so as to meet the practical application.

The paper focuses on research of the influence of the different standardization mode and noise interference for the sub-systems with BP neural network, probability neural network(PNN), radial neural network and Elman neural network methods. Neural network and D-s theory are used to the gas circuit fault diagnosis, and the diagnosis results data fusion is also studied. The simulation experiments manifest that the method is valid and accurate. The results manifest that the standardization of the samples influence the neural network training and anti-noise ability heavily. Equal variance and standardization are feasible optimization methods.

## 2. Standardization and its influence to the neural network training and diagnosis function

### 2.1. Fault diagnosis example and its characteristic sample

Fault diagnosis based on neural network should have large sample tests and training[10]. The sample can be acquired by simulate the engine fault mathematical mode or the practical fault example. The common way

---

E-mail address: gol-tech@hotmail.com

is to combine the two kinds data together[11]. The 12 kinds of fault mode for JT9D engine are analyzed so as to research the multiple neural network modes and their anti-noise ability. The samples of the aeroengine are listed in Tab.1. N1, N2, EGT and FF stand for the FSI of low-voltage rotor speed, high-voltage rotor speed, exhaust temperature and fuel flow respectively.

To make the neural network more feasible and practical for engineering, the training sample can reflect the influence of the random error. The sample with normally distributed random variable is analyzed[12]. The function is as follows:

$$x_{fs} = x_{s0} + k \cdot \sigma \cdot \text{rand}() \quad (1)$$

$\sigma$  is the standard deviation of the measured data,  $k$  is the data dispersion degree,  $x_{s0}$  and  $x_{fs}$  are the ideal input fault mode and simulated fault mode samples,  $\text{rand}()$  is the random number between  $-5 \sim 5$  with gaussian distribution. To compare the diagnosis results of different methods, each fault and the test sample choose 10 samples with gaussian distribution.

## 2.2. Sample standardization

Make normalization processing of the data in the fault samples, and transform all the data in the interval  $[0,1]$ . Thus, the input data can be between the BP network transform function ranges and decrease the error. The common normalization processing methods are range normalization, normal number standardization and unbiased variance normalization [13].

1) Range normalization method. It can be expressed as in function (2).

$$y_i = \frac{X_i - X_{\min}}{X_{\max} - X_{\min}} \quad (i=1,2,\dots,N) \quad (2)$$

$X_i$  is the sample data in  $x=(X_1, X_2, \dots, X_N)$ ,  $N$  is the sample length,  $X_{\max}$ ,  $X_{\min}$  are the max sample and min sample,  $y_i$  is the output of  $X_i$  after normalization.

2) Normal number normalization method. It can be expressed as in function (3)

$$y_j = \frac{X_j}{\text{norm}(X)} = \frac{X_j}{\sqrt{\sum_{i=1}^N X_i^2}} \quad (j=1,2,\dots,N) \quad (3)$$

$X_j$  is the sample data in  $x=(X_1, X_2, \dots, X_N)$ ,  $N$  is the sample length,  $\text{norm}(x)$  is the Euclidean distance of the sample.

3) Unbiased variance normalization. Unbiased variance is to divide the sample data with the standard error to decrease the error influence and then apply normal number normalization in function (3). And this is a feasible normalization method.

## 2.3. Influence of the normalization method to different neural network and fault diagnosis function

This paper builds a three layer BP neural network. And it has 4 neuron for input layer, 10 neuron for middle layer and 12 neuron for output layer. Train the network with different revised algorithms. Table 2 and Table 3 show the diagnosis results of different training method.

Table 2 shows the number of misdiagnosis sample and clarified diagnosis sample. For example “10/134”, its misdiagnosis rate is  $10/144=0.0694$ , and its rate of diagnosis

TABLE I. TYPICAL FAULT SAMPLE AND TWO DIAGNOSIS TEST EXAMPLE OF JT9D AEROENGINE

| No. | Fault mode                             | Input sample: $X_i$    | Output sample: $y(t)$   |
|-----|--|------------------------|---|
|     |  | N1,N2,EGT,FF           | $t_1, t_2, t_3, t_4, t_5, t_6, t_7, t_8, t_9, t_{10}, t_{11}, t_{12}$ |
| 1   | M1(fan efficiency)                     | -0.25,-0.05,-1.0,-0.25 | 1,0,0,0,0,0,0,0,0,0,0   |
| 2   | M2(fan flow)                           | -0.85,0.05,4.5,0.8     | 0,1,0,0,0,0,0,0,0,0,0   |
| 3   | M3(LP motor efficiency)                | 0.1,-0.15,-2.0,-0.15   | 0,0,1,0,0,0,0,0,0,0,0   |
| 4   | M4(LP motor flow)                      | -0.2,-0.05,-2.0,-0.4   | 0,0,0,1,0,0,0,0,0,0,0   |
| 5   | M5(HP motor efficiency)                | -0.1,0.1,-7.0,-0.85    | 0,0,0,0,1,0,0,0,0,0,0   |
| 6   | M6(HP motor flow)                      | 0.0,-0.25,-0.05,-0.1   | 0,0,0,0,0,1,0,0,0,0,0   |
| 7   | M7(HP turbine efficiency)              | -0.1,0.2,-8.5,-1.05    | 0,0,0,0,0,0,1,0,0,0,0   |
| 8   | M8(Area of the HP turbine 1st guider)  | 0.05,-0.15,2.5,0.35    | 0,0,0,0,0,0,0,1,0,0,0   |
| 9   | M9(LP turbine efficiency)              | 0.45,0.0,-4.5,0.0      | 0,0,0,0,0,0,0,0,1,0,0   |
| 10  | M10(Area of the LP turbine 1st guider) | -0.3,0.1,-2.5,-0.6     | 0,0,0,0,0,0,0,0,0,1,0   |
| 11  | M11(HP motor adjustable wing angle)    | 0.0,-0.4,-1.5,-0.15    | 0,0,0,0,0,0,0,0,0,0,1   |

|                        |                                       |                      |                     |
|------------------------|---------------------------------------|----------------------|---------------------|
| 12                     | M12(3.0 blowoff valve can't turn off) | 0.0,1.0,25.0,4.5     | 0,0,0,0,0,0,0,0,0,1 |
| Diagnosis test example | TA40(HP turbine wing broken)          | 0.2, -1.3, 18.2, 3.8 | TA40 with M8 fault; |
|                        | CL16 (3.0 blowoff valve leakage)      | 0.2, 0.6, 14.3, 3.2  | CL16 with M12 fault |

TABLE II. MEASUREMENT RESULT WITH UNBIASED VARIANCE NORMALIZATION

| Noise intensity | Trainrp (6.672s) |        | Traincgrf (7.688s) |        | Trainlm (10.016s) |        | Trainscgr(15.375s) |       | Traingdx(803.321s) |        | Traingdm(3183.859s) |       |
|-----------------|------------------|--------|--------------------|--------|-------------------|--------|--------------------|-------|--------------------|--------|---------------------|-------|
|                 | TA40             | CL16   | TA40               | CL16   | TA40              | CL16   | TA40               | CL16  | TA40               | CL16   | TA40                | CL16  |
| 0.0 %           | 0/144            | 0/144  | 0/144              | 0/144  | 0/144             | 0/144  | 0/144              | 0/144 | 0/144              | 0/144  | 0/144               | 0/144 |
| 1.0 %           | 0/144            | 0/144  | 0/144              | 0/144  | 0/144             | 0/144  | 0/144              | 0/144 | 0/144              | 0/144  | 0/144               | 0/144 |
| 2.0 %           | 0/144            | 0/144  | 0/144              | 2/142  | 0/144             | 0/144  | 0/144              | 0/144 | 0/144              | 0/144  | 0/144               | 0/144 |
| 3.0 %           | 0/144            | 0/144  | 4/140              | 25/119 | 0/144             | 0/144  | 1/143              | 0/144 | 0/144              | 0/144  | 1/143               | 0/144 |
| 5.0 %           | 4/140            | 23/121 | 12/132             | 45/99  | 24/120            | 13/131 | 16/128             | 5/139 | 24/120             | 13/131 | 16/128              | 5/139 |

TABLE III. MEASUREMENT RESULT WITH RANGE NORMALIZATION

| Noise intensity | Trainrp(52.391s) |       | Trainlm (72.391s) |       | Trainscgr(212.203s) |       | Traincgrf(213.328s) |        | Traingdx(864.297s) |        | Traingdm(3661.656s) |        |
|-----------------|------------------|-------|-------------------|-------|---------------------|-------|---------------------|--------|--------------------|--------|---------------------|--------|
|                 | TA40             | CL16  | TA40              | CL16  | TA40                | CL16  | TA40                | CL16   | TA40               | CL16   | TA40                | CL16   |
| 0.0 %           | 0/144            | 0/144 | 0/144             | 144/0 | 0/144               | 0/144 | 0/144               | 0/144  | 0/144              | 0/144  | 0/144               | 0/144  |
| 1.0 %           | 4/140            | 79/65 | 11/13             | 104/3 | 0/144               | 67/77 | 0/144               | 0/144  | 15/129             | 6/138  | 1/143               | 8/136  |
| 2.0 %           | 23/121           | 52/92 | 56/88             | 70/74 | 1/143               | 73/71 | 10/134              | 72/72  | 42/102             | 42/102 | 14/130              | 72/72  |
| 3.0 %           | 45/99            | 68/76 | 50/94             | 70/74 | 30/114              | 73/71 | 15/129              | 91/53  | 79/65              | 77/70  | 50/94               | 89/55  |
| 5.0 %           | 78/66            | 64/80 | 110/3             | 80/64 | 31/113              | 89/59 | 51/93               | 104/40 | 106/38             | 93/51  | 40/104              | 121/23 |

accuracy is  $134/144 * 100\% = 93.6\%$ , Train(X,X) stand for MATLAB training function mode. By comparing the results, the result of unbiased variance normalization is better than range normalization, with higher training speed and better anti-noise ability. The ideal diagnosis accuracy is next to 100%. With the increase of noise, the misdiagnosis rate arises.

### 3. Construction of the fault diagnosis system for aeroengine based on neural network and D-s theory

#### 3.1.Data fusion diagnosis system structure

The fault diagnosis system for aeroengine is shown in Fig.1. It consists of BP neural network, PNN neural network, Elman neural network and RBF neural network fault diagnosis sub-system, and the D-s evidence data fusion subsystem.

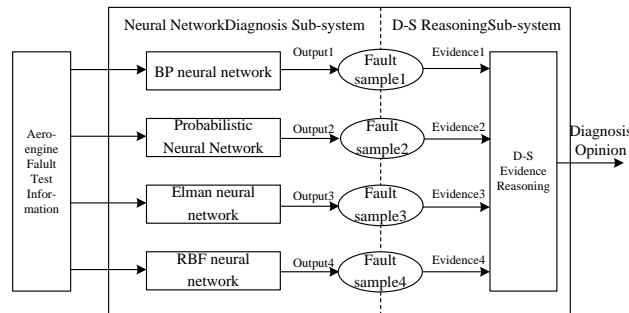


Figure 1. Diagnosis system structure

#### 3.2.Evidence diagnosis sub system based on neural network

In the data fusion diagnosis system, the diagnosis result of each neural network sub system is the input evidence for the data fusion diagnosis system, also called evidence diagnosis acquisition sub system.

##### 1) Evidence1 BP neural network fault diagnosis sub system

BP neural network is a feed-forward network, it has a layered structure. Each layer consists of units which receive their input from units from a layer directly below and send their output to units in a layer directly

above the unit. This paper applies the Trainlm of Levenberg-Marquardt, batch processing training mode, with  $4 \times 10 \times 12$  three layer structure and logsig transform function, train the network by pattern classifier.

2) Evidence 2 Probabilistic Neural Network fault diagnosis sub system

Probabilistic Neural Networks are forward feed networks built with three layers. They are derived from Bayes Decision Networks. They train quickly since the training is done in one pass of each training vector, rather than several. Probabilistic neural networks estimate the probability density function for each class based on the training samples. It has the features as quick training speed, good anti-noise ability and high diagnosis accuracy.

3) Evidence 3 Elman neural network fault diagnosis sub system

Elman network commonly is a two-layer network with feedback from the first-layer output to the first-layer input. This recurrent connection allows the Elman network to both detect and generate time-varying patterns. The Elman network has tansig neurons in its hidden layer, and purelin neurons in its output layer. This combination is special in that two-layer networks with these transfer functions can approximate any function with arbitrary accuracy. This paper applies the Trainrp, batch processing training mode. It has the features as quick training speed, good anti-noise ability and high diagnosis accuracy than BP neural network.

4) Evidence 4 RBF neural network fault diagnosis sub system

Radial Basis Function(RBF) neural network has an input layer, a hidden layer and an output layer. The neurons in the hidden layer contain Gaussian transfer functions whose outputs are inversely proportional to the distance from the center of the neuron. This paper applies radbas function and the spread set 2.

**3.3.Diagnosis strategy fusion sub system based on D-S theory**

D-S evidence theory express the proposition with set, and build on the nonempty set  $\Omega$ .  $\Omega$  is the basic fault sample, it has  $2^\Omega$  kind of combinations. The elementary probability distribution function M is shown in function (4).

$$M:2^\Omega \rightarrow [0,1], \text{ and meet } M(\Phi) = 0, \sum M(A) = 1 \tag{4}$$

$\Phi$  is the empty set, A is a random proposition, it's a subset of  $\Omega$ . In fault diagnosis A stand for the possible fault, M(A) is the elementary probability of A,  $\{A, M(A)\}$  is the evidence volume.

Make data fusion for the initial fault diagnosis based on these for sub systems with D-S theory, and test the 12 kind fault mode of the aeroengine gas circuit components. To get the M elementary probability function of each fault mode becomes important. Paper applies the follow method to build M: The evidence volume  $E_i$  is an eigenvector  $X_i = \{x_i^1, x_i^2, \dots, x_i^N\}, i=1,2,3,4$  and the proposition  $F_j$  the eigenvalue is the standard vector  $Y_{ji} = \{y_{ji}^1, y_{ji}^2, \dots, y_{ji}^N\}, i = 1,2,3,4; j = 1,2, \dots, 12$ , then the angular cosine distance is

$$d_{ij} = (X_i, Y_{jt}) = \cos(\theta) = \frac{X_i^T Y_{jt}}{\|X_i\| \cdot \|Y_{jt}\|} \tag{5}$$

The M elementary probability function is

$$M_i(A_j) = \frac{(d_{ij} + \alpha)^{-1}}{\sum_{j=1}^{12} (d_{ij} + \alpha)^{-1}} \tag{6}$$

$\alpha$  is the modifying factor and its value  $\alpha < 10^{-4}$ .

**4. Simulation and Measurement Result Analysis**

**4.1.Simulation and Measurement Result**

Apply the sample after unbiased variance normalization, build four neural networks, train, test the networks, apply D-S theory to make strategy fusion and get the final fault diagnosis result shown in Table 4.

**4.2.Analysis of the diagnosis result**

In Table 4, test the random sample under each noise for 100 times. The number in the unit form stands for the number of misdiagnosis sample and clarified diagnosis sample, and can get the rates.

TABLE IV. TA40 AND CL16 FAULT DIAGNOSIS RESULTS

| SNR | 0.0% |     | 1.0% |     | 3.0% |     | 5.0% |     | 7.0% |     | 10.0% |      |
|-----|------|-----|------|-----|------|-----|------|-----|------|-----|-------|------|
|     | TA4  | CL1 | TA4  | CL1 | TA4  | CL1 | TA4  | CL1 | TA4  | CL1 | TA4   | CL16 |
|     | 0    | 6   | 0    | 6   | 0    | 6   | 0    | 6   | 0    | 6   | 0     |      |

|                                |      |      |      |      |       |       |       |       |       |       |       |       |
|--------------------------------|------|------|------|------|-------|-------|-------|-------|-------|-------|-------|-------|
| BP sub-system                  | 0/10 | 0/10 | 0/10 | 0/10 | 24/76 | 0/10  | 57/43 | 57/43 | 90/10 | 19/81 | 97/3  | 26/74 |
| PNN sub-system                 | 0/10 | 0/10 | 0/10 | 0/10 | 16/84 | 0/10  | 0/100 | 0/100 | 1/99  | 0/10  | 40/60 | 32/68 |
| Elmax sub-system               | 0/10 | 0/10 | 0/10 | 0/10 | 47/53 | 1/99  | 0/10  | 51/49 | 0/10  | 56/44 | 26/74 | 62/38 |
| RBF sub-system                 | 0/10 | 0/10 | 0/10 | 0/10 | 49/51 | 19/81 | 94/6  | 79/21 | 92/8  | 95/5  | 95/5  | 87/13 |
| BP&PNN fusion output           | 0/10 | 0/10 | 0/10 | 0/10 | 16/84 | 0/10  | 52/48 | 0/10  | 72/28 | 0/10  | 90/10 | 29/71 |
| BP&PNN&Elmax fusion output     | 0/10 | 0/10 | 0/10 | 0/10 | 16/84 | 0/10  | 40/60 | 0/10  | 18/82 | 1/99  | 87/13 | 29/71 |
| BP&PNN&Elma& RBF fusion output | 0/10 | 0/10 | 0/10 | 0/10 | 16/84 | 0/100 | 39/61 | 0/100 | 18/82 | 0/100 | 88/12 | 29/71 |

When signal noise ratio(SNR) is small than 1%, all the diagnosis rate is 100%, and without any misdiagnosis. Among all the results, PNP has the best diagnosis rate and anti-noise ability. When SNR is small is big than 3, the diagnosis rates of TA40 and CL16 are different, they can express with the average diagnosis rate.

Figure shows the average diagnosis rates curves of TA40 and CL16. With the increase of noise intensity, the fault diagnosis rate decrease, therefore the misdiagnosis rate becomes bigger. After the D-S theory fusion, the diagnosis rate is improved, and also the anti-noise ability is improved.



Figure2. Average diagnosis rate for TA40 and CL16

## 5. Conclusion

This paper discusses the fusion algorithm based on Dempster-Shafer theory of evidence and neural networks. The standardization of the samples influences the neural network training and anti-noise ability heavily. Equal variance and standardization are feasible optimization methods. PNN has the features as quick training speed, good anti-noise ability and high diagnosis accuracy. The training of PNN got the best diagnosis rate.

Compared with the approaches that only adopt D-S evidence theory or neural networks, the accuracy of diagnostic results is obviously improved. It improves the system function, the validity and accuracy of fault diagnosis for the aeroengine.

## 6. Acknowledgment

The work of the paper was finished in China Gas Turbine Establishment, thank the researcher XingZhang Wu and my colleagues there.

## 7. References

- [1] Liao Wei, Wang Hua, Han Pu, "Neural network modeling of aircraft power plant and fault diagnosis method using time frequency analysis", Control and Decision Conference, 2009. CCDC '09. Jun, 2009, pp353-356.I
- [2] Wu W J, Qing D X. "Research on Timesynchronization Based Test Instrumentation and Control System of Aeroengine", Gas Turbine Experiment And Research , Vol 02, 2004, pp35-37.

- [3] Roemer,M.J;Orsaghy,R.F;Schoeller,M;etal. “Upgrading engine test cells for improved troubleshooting and diagnostics”, 2002 Aerospace conference proceedings,2002.IEEE,pp.5-13.
- [4] Urban L A.”Gas Path Analysis Applied to Turbine Engine Condition Monitoring”,AIAA Paper No.72-1082,1972
- [5] Cai, K. Sun, Y. Yao, “Fault Diagnosis and Adaptive Reconfiguration Control for Sensors in Aeroengine”, Electronics, Optics & Control. Vol. 16, no. 6, June 2009, pp. 57-61.
- [6] Zhou Genna, Hou Shengli, Bo Lin, Shi Xiaopei, WangWei, “Fault Diagnosis of Rotor System Based on Wavelet Energy Immune Recognition”, Electronics, Optics & Control. Vol. 17, no. 6, Jun 2010, pp. 81-84.
- [7] Hou Shengli, Wang Wei, Qiao Li, Shi Xiaopei, Zhou Genua, “Feature Extraction and Multi-Sensor Fault Diagnosis Based on Clonal Clustering”, Electronics, Optics & Control. Vol. 17, no. 6, 88. Jun 2010, pp. 69-72.
- [8] Zhao ting yu, “Aeroengine’s mathematical mode”, Journal of UESTC of China, Vol 34, No. 4, Aug,2005, pp 545-547.
- [9] Dungen Chen, Guangbin Ding, ”Multi-concurrent fault diagnosis approach for aeroengine based on wavelet fuzzy network”, Control and Decision Conference, 2009. CCDC '09, 17-19 June 2009 On page(s): 5421 – 5426.
- [10]Liao Wei, Han Pu, “Wavelet neural network aided on-line detection and diagnosis of rotating machine fault”, Control and Decision Conference, 2008, pp1868 – 1871.
- [11]Liao Wei, Wang Hua,Han Pu, “ Neural network modeling of aircraft power plant and fault diagnosis method using time frequency analysis” Control and Decision Conference, 2009. CCDC '09, pp 353 – 356.
- [12]Li-Ying Jiang; Yan Zhang; Zhong-Hai Li; Yi-Bo Li;” Aero-engine fault diagnosis based on multi-scale Independent Component Analysis”, Wavelet Analysis and Pattern Recognition, 2009. ICWAPR 2009. Page(s): 118 – 122.
- [13]Rui Zhu, Dezhi Wu, Zhirong Liu, Xinye Wu, Yinbiao Guo, “Aeroengine modules performance deterioration modeling and assessment”, 2010 IEEE International Conference on Industrial Engineering and Engineering Management (IEEM), pp1626 -1630.